Journal of the Iranian Chemical Society (2018) 15:431–443
https://doi.org/10.1007/s13738-017-1244-4

ORIGINAL PAPER

Nanoparticles of manganese oxides as efficient catalyst for the synthesis of pyrano[2,3-*d*]pyrimidine derivatives and their complexes as potent protease inhibitors

Wesam S. Shehab[1] · **Walaa H. El-Shwiniy**[1]

Received: 6 July 2017 / Accepted: 14 November 2017 / Published online: 30 November 2017

Abstract
Novel pyrano[2,3-*d*] pyrimidine derivatives were synthesized via the three-component reaction of thiophene-2-carbaldehyde, malononitrile and barbituric or thiobarbituric acid in the presence of Mn_2O_3 nanoparticles. This method has been found to be eco-friendly and economical. Compound **1** was used as a precursor for the synthesis of new pyranopyrimidine derivatives **2–5**. Moreover, 7-amino-2,3,4,5-tetrahydro-4-oxo-5-(thiophen-2-yl)-2-thioxo-1H-pyrano[2,3-d]pyrimidine-6-carboxamide **4** was then converted into another set of novel compounds **6–8**. On the other hand, a series of Mn(II) complexes with pyrano[2,3-*d*] pyrimidine derivatives have been prepared. The synthesized compounds and its complexes were characterized by elemental analysis, magnetic and spectroscopic methods (IR, XRD, SEM, TEM, ^{13}C, $^{1}HNMR$) as well as thermal analysis. The spectrophotometric determinations suggest a distorted octahedral geometry for all complexes. The organic compounds and its chelates as inhibitors exhibited remarkable effects on the enzyme activity of an extracellular toxic protease, KB76 from *Brevibacterium otitidis* as well as against different bacterial and fungal strains.

Keywords Nanocatalyst · Multicomponent reactions · Pyrano[2,3-d]pyrimidine derivatives · PIS · Complexes · Spectral study

Introduction

A major challenge of the modern synthetic chemistry is to design highly efficient chemical reaction sequences which provide molecules containing maximum complexity and structural diversity with interesting bioactivities in minimum number of synthetic steps. In recent times, multicomponent reactions (MCRs) have become progressively attractive tools for the fast preparation of compound libraries of small molecules [1, 2].

Pyrano[2,3-d]pyrimidine is unsaturated six-membered heterocycle which is formed by fusion of pyran and pyrimidine rings together, consisting of one oxygen atom at position number 8 and two nitrogen atoms at position numbers 1 and 3, respectively. If pyrano[2,3-d]pyrimidine moieties are clubbed into one molecule, then resultant derivative enhances its pharmaceutical activity as abundant in biologically active compounds such as antitumor [3], cardiotonic [4], antibronchitic [5] and antifungal activity [6]. Pyrano[2,3-d]pyrimidines are building blocks used to evaluate their antimicrobial activities, and various derived natural products are also used as a drug for insomnia treatment [7]. Therefore, for the preparation of these complex molecules large efforts have been directed toward the synthetic manipulation of pyrano[2,3-d]pyrimidine derivatives. Pyrano[2,3-d] pyrimidine synthesis was reported under various conditions such as microwave irradiation [8, 9], ultrasonic irradiation [10], solvent-free condition and in aqueous medium in the absence of catalysts [11].

Nowadays, metal nanoparticles and functionalized magnetic nanoparticles, especially supported superparamagnetic metal nanoparticles, have attracted considerable interest in both academic and industrial researches because of their potential applications in chemical, biomedical and materials science. As a result, they have enabled researchers to

Electronic supplementary material The online version of this article (https://doi.org/10.1007/s13738-017-1244-4) contains supplementary material, which is available to authorized users.

✉ Wesam S. Shehab
wsshehab@zu.edu.eg; wesamshehab2015@gmail.com

[1] Department of Chemistry, Faculty of Science, Zagazig University, Zagazig 44519, Egypt

apply nanocatalysts as greener and sustainable options for organic transformations [12–22]. Reaction with metal ions had some serious effect for the solubility, pharmacokinetics and bioavailability of the synthesized organic compounds and is also implicated in the mechanism of action of these bactericidal and fungicidal agents [23].

Herein, we have developed a new synthetic route for the one-pot three-component synthesis of annulated fused pyrano[2,3-d]pyrimidines **1,1a** in the presence of Mn_2O_3 nanoparticles. This has prompted us to see whether this reaction can be utilized as one of the bases for producing condensed pyrimidines in connection to our interest in the chemistry of condensed pyrimidines [14, 24–27] and synthesize novel Mn(II) complexes to improve efficacy or stability and also, on the activity of biological properties also, to determine the target sites of novel synthesized compounds an extracellular toxic protease, KB76 from *Brevibacterium otitidis*. For the characterization of the compounds the following spectroscopic and analytical techniques were employed: elemental analyses, IR, ^{1}H, ^{13}CNMR, electronic spectra and magnetic moment as well as thermogravimetric analysis.

Experimental

Materials and instrumentation

Thiophene-2-carbaldehyde, malononitrile, manganese chloride ($MnCl_2{\cdot}4H_2O$) were purchased from Sigma-Aldrich Company, ammonium hydrogen carbonate (NH_4HCO_3) was supplied by Fluka Company, and all solvents were purchased from El-Nasr Pharmaceutical Chemicals Company (analytical reagent grade, Egypt). Barbituric acid and 2-thiobarbituric acid were purchased from Central Laboratory of Health Ministry. All chemicals were used as supplied without further purification.

C, H and N analysis was carried out on a PerkinElmer CHN 2400. The percentages of the metal ions were determined gravimetrically by transforming the solid products into metal oxide. The percentages of the metal ions were also estimated using an atomic absorption spectrometer. The spectrometer model was Pye-Unicam SP 1900 and fitted with the corresponding lamp. IR spectra were recorded on FT-IR 460 PLUS (KBr disks) in the range from 4000 to 400 cm^{-1}. ^{1}H and ^{13}C NMR spectra were recorded on a Bruker 300 MHz NMR Spectrometer using tetramethylsilane (TMS) as the internal standard, chemical shifts are expressed in δ (ppm), and DMSO-*d*6 was used as the solvent. TGA–DTG measurements were taken with heating rate of 20 ^{o}C min^{-1} under N_2 atmosphere from room temperature to 800 ^{o}C using TGA-50H, Shimadzu. The mass of sample was accurately weighted out in an aluminum crucible. Scanning electron microscopy (SEM) images were taken in Quanta FEG 250 equipment. The X-ray diffraction patterns (XRD) were obtained on Pikagu diffractometer using Cu/Kα radiation. Absorbance measurements were conducted on a double-beam spectrophotometer (T80 UV/Vis) with wavelength range 190–1100 nm, spectral bandwidth of 2 nm. Magnetic measurements were taken on a Sherwood scientific magnetic balance using Gouy balance using $Hg[Co(SCN)_4]$ as calibrant. All melting points are uncorrected and were determined on a Gallen Kamp electric melting point apparatus. Molar conductivities of the solutions of the ligand and metal complexes in DMSO with concentrations of 1×10^{-3} M were measured on CONSORT K410. The completion of the reactions was confirmed using thin-layer chromatography (TLC) on silica gel-coated aluminum sheets.

Synthesis

General procedure for synthesis of pyrano[2,3-*d*]pyrimidine derivatives

A solution of thiophene-2-carbaldehyde(1 mmol), malononitrile (1 mmol), barbituric or thiobarbituric acid (1 mmol) of ethanol, the presence of a catalytic amount of supported metal nanoparticles Mn_2O_3 (1 mmol). After completion of the reaction, the catalyst was removed by using an external magnet and the solid product was collected by filtration and washed with ethanol. We do not investigate the catalytic activity and promising properties with respect to their nanocatalyst leaching or degradation behavior during recycling.

7-Amino-4-oxo-2-sulfanylidene-5-(thiophen-2-yl)-1,3,4,5-tetrahydro-2*H*-pyrano[2,3-*d*]pyrimidine-6-carbonitrile (1 = L_2) Pale yellow solid, yield 82%, m.p. 117.38 °C. IR (KBr, *v*, cm^{-1}): 3431, 3200 (NH_2), 3146, 3049 (2NH), 2228 (CN), 1694 (CO) and 1256 cm^{-1}(C=S). δ = ^{1}H NMR (DMSO-*d*6, 300 MHz): δ = 3.36 (s, 1H, H-5), 7.26 (s, 2H, NH_2), 7.28 (d, 1H, J = 3.6 Hz, thienyl-C_3'H), 7.94 (dd, 1H, thienyl-C_4'H), 8.11 (d, 1H, J = 5.2 Hz, thienyl-C_5'H), 11.38,13.17 (2 s, 2H, NH exchangeable by D_2O); ^{13}C NMR (DMSO-*d*6, 150 MHz): δ = 35.7, 57.5, 86.58, 116.2, 124.3, 130.7, 146.4, 149.6151.9, 152.7, 157.8, 162.6176.6 ppm. Anal. Calcd for $C_{12}H_8N_4O_2S_2$ (304.01): C, 47.36; H, 2.65; N, 18.41; S, 21.07; Found C, 47.39; H, 2.69; N, 18.45; S, 21.09%.

7-Amino-2,3,4,5-tetrahydro-2,4-dioxo-5-(thiophen-2-yl)-1*H*-pyrano[2,3-*d*]pyrimidine-6-carbonitrile (1a = L_1) Pale yellow solid; yield 85%; m.p = 158.57 °C; IR (KBr, *v*, cm^{-1}): 3490–3385 cm^{-1} (NH_2), 3174 (2NH br), 2222 cm^{-1} (CN), 1677, 1648 cm^{-1} (2C=O) and 1258 cm^{-1}(C–O). ^{1}H NMR (DMSO-d_6,

300 MHz): $\delta = 3.36$ (s, 1H, H-5), 7.26 (s, 2H, NH_2), 7.28(d, 1H, $J = 3.6$ Hz, thienyl-C_3'H), 7.94 (dd, 1H, $J = 4.2$, thienyl-C_4'H), 8.11 (d, 1H, $J = 5.2$ Hz, thienyl-C_5'H), 11.12,12.17 (2 s, 2H, NH exchangeable by D_2O); ^{13}CNMR (DMSO-*d*6, 150 MHz): $\delta = 35.7$, 57.5, 86.58, 116.2, 124.3, 130.7, 146.4, 149.6151.9, 152.7, 157.8, 162.6 ppm. Anal. Calcd for $C_{12}H_8N_4O_3S$ (288.03): C, 50.00; H, 2.80; N, 19.43; S, 11.12; Found C, 50.02; H, 2.82; N, 19.45; S, 11.20%.

[6-Amino-4-oxo-2-sulfanylidene-5-(thiophen-2-yl)-1,3,4,5-tetrahydro-2*H*-pyrano[2,3-*d*:6,5-*d'*]dipyrimidin-8-yl]acetonitrile (2) A mixture of (**1**) (20 mmol) and malononitrile (20 mmol) was added to 20 mL freshly prepared sodium ethoxide solution [prepared by adding 1.0 g sodium metal into absolute ethanol (20 mL)], and the mixture was refluxed for 7 h and left to cool overnight. The solid product was collected by filtration and washed and recrystallized with ethanol. Pale yellow crystals; m.p = 226.95 °C; yield 77%; IR (KBr, *v*, cm^{-1}): 3463 and 3296 (NH_2), 2213 (CN) cm^{-1} and 1261 cm^{-1}(C=S). ^{1}H NMR (DMSO-d_6, 300 MHz): $\delta = 3.36$ (s, 1H, H-5), 4.17 (s, 2H, CH_2), 7.28 (d, 1H, $J = 3.6$ Hz, thienyl-C_3'H), 7.79 (dd, 1H, $J = 3.6$, thienyl-C_4'H), 7.91 (d, 1H, $J = 5.2$ Hz, thienyl-C_5'H), 8.00 (br s, 2H, NH_2), 11.38,13.17 (2 s, 2H, NH). Anal. Calcd for $C_{15}H_{12}N_6O_2S_2$ (372.05): C, 48.38; H, 3.25; N, 22.57; S, 17.22; Found C, 48.36; H, 3.26; N, 22.58; S, 17.20%.

2-Sulfanylidene-5-(thiophen-2-yl)-5,7-dihydro-2*H*-pyrano[2,3-*d*:6,5-*d'*]dipyrimidine-4,6(1*H*,3*H*)-dione (3) Compound **1** (10 mmol) was heated under reflux conditions in formic acid (30 mL, 85%) for 8 h. The reaction mixture was cooled and poured into ice-cold water. The formed solid was filtered off, dried and recrystallized from dimethylformamide to give compound **3**. Pale brown crystals of mp = 135.78 °C; yield 65%; IR (KBr, *v*, cm^{-1}): 3435 (NH), 3126 (NH), 1672 (C=O cm^{-1}) and 1258 cm^{-1}(C=S). ^{1}H NMR (DMSO-*d*6, 300 MHz): $\delta = 3.36$ (s, 1H, H-5), 7.37 (d, 1H, $J = 3.6$ Hz, thienyl-C_3'H), 7.40 (dd, 1H, $J = 3.5$, thienyl-C_4'H), 8.13 (d, 1H, $J = 5.2$ Hz, thienyl-C_5'H), 12.35, 13.37 (br, 3H, NH).Anal. Calcd for $C_{13}H_8N_4O_3S_2$ (332.36): C, 46.98; H, 2.43; N, 16.86; S, 19.30; Found C, 46.97; H, 2.41; N, 16.85; S, 19.30%.

7-Amino-4-oxo-2-sulfanylidene-5-(thiophen-2-yl)-1,3,4,5-tetrahydro-2*H*-pyrano[2,3-*d*]pyrimidine-6-carboxamide (4) To (10 mmol) of compound **1**, cold concentrated sulfuric acid (10 mL) was added portionwise with ice bath cooling and stirring. After 10 min, the ice bath was removed and the mixture was stirred for an additional 15 min. The resulting pale yellow solution was carefully poured onto crushed ice, and the resulting precipitate was collected, washed with water, dried and recrystallized from dioxane to give compound **4.** Yellow crystals of mp = 176–178 °C; yield 60%; IR (KBr, *v*, cm^{-1}): 3431 (NH_2), 3126 (NH_2), 3114 (NH), 1671,1645 (2C=O) and 1256 cm^{-1}(C=S).^{1}H NMR (DMSO-d_6, 300 MHz): $\delta = 3.36$ (s, 1H, H-5), 7.37(d, 1H, $J = 3.6$ Hz, thienyl-C_3'H), 7.40 (dd, 1H, $J = 3.5$, thienyl-C_4'H), 8.13 (d, 1H, $J = 5.2$ Hz, thienyl-C_5'H),8.48 (s, 2H, D_2O Exch., NH_2), 9.14 (s, 2H, D_2O Exch., NH_2), 12.37 (s, 1H, D_2O Exch., pyrimidine NH). Anal. Calcd for $C_{12}H_{10}N_4O_3S_2$ (322.02): C, 44.71; H, 3.13; N, 17.38; S, 19.89; Found C, 44.70; H, 3.12; N, 17.39; S, 19.88%.

6-Amino-2-sulfanylidene-5-(thiophen-2-yl)-1,2,3,5-tetrahydro-4*H*-pyrano[2,3-*d*:6,5-*d'*]dipyrimidin-4-one (5) A mixture of compound **1** (10 mmol) and formamide (30 mL) was heated at 150 °C for 3 h. The reaction mixture was cooled and poured into water. The formed solid was filtered off, dried and recrystallized from ethanol to afford compound **5** as pale brown crystals mp = 255.45 °C, yield 67%; IR (KBr, *v*, cm^{-1}): 3423 (NH_2), 3190 (NH),1683(C=O) and 1250 (C=S) cm^{-1}. ^{1}H NMR (DMSO-d_6, 300 MHz): $\delta = 3.36$ (s, 1H, H-5), 7.37(d, 1H, $J = 3.6$ Hz, thienyl-C_3'H), 7.40 (dd, 1H, $J = 3.5$, thienyl-C_4'H), 7.93 (s, 1H, D_2O Exch., NH_2), 8.23 (s, 1H, pyrimidine), 8.34 (d, 1H, $J = 5.2$ Hz, thienyl-C_5'H), 12.35,12.37 (2 s, 2H, NH). Anal. Calcd for $C_{13}H_9N_5O_2S_2$ (331.02): C, 47.12; H, 2.74; N, 21.13; S, 19.35; Found C, 47.13; H, 2.72; N, 21.12; S, 19.37%.

5-Thiophen-2-yl-2,8-dithioxo-2,3,5,7,8,9-hexahydro-1*H*-pyrano[2,3-d;6,5-*d'*]dipyrimidine-4,6-dione (6) To a solution of compound **4** (10 mmol) in dimethylformamide (30 mL), 20% potassium hydroxide solution (potassium hydroxide 1.68 g, water 7 mL) and carbon disulfide (5 mL) were added. The reaction mixture was heated under reflux for 15 h, then poured into water and filtered off. The filtrate was precipitated with HCl (0.1 N), and the solid product was collected, washed with water, dried and recrystallized from ethanol to give pale brown crystals of compound **6.** mp = 297.11 °C, yield 68%. IR (KBr, *v*, cm^{-1}): 3431 (NH), 3216 (NH), 3089 (NH), 1670, 1651 (2C=O) and 1254 cm^{-1}(C=S). ^{1}H NMR (DMSO-d_6, 300 MHz): $\delta = 3.36$ (s, 1H, H-5), 7.37(d, 1H, $J = 3.6$ Hz, thienyl-C_3'H), 7.40 (dd, 1H, $J = 3.6$, thienyl-C_4'H), 8.34 (d, 1H, $J = 5.2$ Hz, thienyl-C_5'H), 8.90 (s, 1H, D_2O Exch., NH), 9.93 (s, 1H, D_2O Exch., NH), 11.67 (s, 1H, D_2O Exch., NH). Anal. Calcd for $C_{13}H_8N_4O_3S_3$ (363.98): C, 42.85; H, 2.21; N, 15.37; S, 26.40; Found C, 42.84; H, 2.20; N, 15.37; S, 26.41%.

10-Thiophen-2-yl-7-thioxo-4a,6,7,8,9a,10-hexahydro-3*H*-9-oxa-1,2,3,6,8-pentaaza-anthracene-4,5-dione (7) To a suspended solution of compound **4** (10 mmol) in concentrated hydrochloric acid (30 mL) at 0–5 °C, a solution of sodium nitrite (3.00 g) in water (5 mL) was

added over 20 min. After 2 h of stirring at room temperature, the foamy mixture was filtered off. The resulting solid was washed with ice-cold water, dried and recrystallized from ethanol to give pale brown crystals of compound **7** mp = 150–152 °C, yield 64% IR (KBr, *v*, cm^{-1}): 3226 (NH), 3118 (NH), 1675 (C=O) and 1254 cm^{-1}(C=S). ^{1}H NMR (DMSO-d_6, 300 MHz): δ = 3.36 (s, 1H, H-5), 7.37(d, 1H, *J* = 3.6 Hz, thienyl-C_3'H), 7.40 (dd, 1H, *J* = 3.5, thienyl-C_4'H), 8.34 (d, 1H, *J* = 5.2 Hz, thienyl-C_5'H), 8.90 (s, 1H, D_2O Exch., NH), 9.93 (s, 1H, D_2O Exch., NH), 10.78 (s, 1H, D_2O Exch., NH).Anal. Calcd for $C_{12}H_9N_5O_3S_2$ (335.36): C, 42.98; H, 2.70; N, 20.88; S, 19.12; Found C, 42.97; H, 2.70; N, 20.87; S, 19.11%.

6-Hydroxy-5-thiophen-2-yl-2-thioxo-1,2,3,5-tetrahydro-pyrano[2,3-*d*;6,5-*d*′]dipyrimidin-4-one (8) A mixture of compound **4** (10 mmol) and formamide (30 mL) was heated at 150 °C for 3 h. The reaction mixture was cooled and poured into water. The formed solid was filtered off, dried and recrystallized from ethanol to afford pale brown crystals of compound **8**. mp = 288–290 °C, yield 67% IR (KBr, *v*, cm^{-1}): 3226 (NH), 3179 (br, OH), 1680 (C=O) cm^{-1} and 1250 cm^{-1}(C=S). ^{1}H NMR (DMSO-d_6, 300 MHz): δ = 3.36 (s, 1H, H-5), 7.37(d, 1H, *J* = 3.6 Hz, thienyl-C_3'H), 7.40 (dd, 1H, *J* = 3.7, thienyl-C_4'H), 8.00 (d, 1H, *J* = 5.2 Hz, thienyl-C_5'H), 8.07 (s, 1H, pyrimidine), 10.78,11.37 (2 s, 2H, NH), 12.46 (br s, 1H, OH). Anal. Calcd for $C_{13}H_8N_4O_3S_2$ (332.36): C, 46.98; H, 2.43; N, 16.86; S, 19.30; Found C, 46.98; H, 2.42; N, 16.87; S, 19.31%.

Synthesis of metal complexes

The complexes have been synthesized by direct reaction between L_1 and L_2 ligands and manganese chloride. The $[Mn(L_1)(H_2O)Cl_2]$ and $[Mn(L_2)(H_2O)Cl_2]$ complexes were synthesized as follows: 1 mmol (0.197 g) of $MnCl_2{\cdot}4H_2O$ dissolved in 5 mL double-distilled water was added to a magnetically stirring solution containing 1 mmol (0.304 and 0.288 g) L_1 and L_2 in 25 mL acetone. The mixtures were stirred at room temperature for 12 h. The mixture was left for slow evaporation to concentrate the reaction mixture; the yellowish white and lemon yellow precipitates formed were filtered off, washed several times with double-distilled water and dried over $CaCl_2$ in a desiccator under vacuum.

$[Mn(L_1)(H_2O)Cl_2]$ Color: yellowish white; yield: 97%; m.p.: 325.27 °C; M.Wt: 448.29; elemental analysis: found, C 32.33%, H 2.09%, N 12.52%, M 12.76%. Calc. for $MnC_{12}H_{10}N_4O_3S_2Cl_2$, C 32.16%, H 2.25%, N 12.50%, Mn 12.26%; Λ_m = 7.00 S cm^2 mol^{-1}; IR (KBr, *v*, cm^{-1}): 3431 m, 3200 m (NH_2), 2228w (CN), 1654vs (C=O), 754 ms (ring deformation), 609vs (M–O) and 515vs (M–N). δ = ^{1}H NMR (DMSO-*d*6, 300 MHz): δ = 3.36 (s, 1H, H-5), δ = 4.10 (s, 2H, H_2O), 7.26 (s, 2H, NH_2), 7.28 (d, 1H, *J* = 3.6 Hz, thienyl-C_3'H), 7.94 (dd, 1H, *J* = 3.5, thienyl-C_4'H), 8.11 (d, 1H, *J* = 5.2 Hz, thienyl-C_5'H), 10.25 (s, 1H, N–H coordinated) and 13.15 (s, 1H, N–H free).

$[Mn(L_2)(H_2O)Cl_2]$ Color: lemon yellow; yield: 87%; m.p.: 203.89 °C; M.Wt: 432.14; elemental analysis: found, C 32.33%, H 2.09%, N 12.52%, M 12.76%. Calc. for $MnC_{12}H_{10}N_4O_4SCl_2$, C 33.35%, H 2.33%, N 12.96%, Mn 12.71%; Λ_m = 9.70 S cm^2 mol^{-1}; IR (KBr, *v*, cm^{-1}): 3490 m, 3385 m (NH_2), 2222 ms (CN), 1664vs (C=O), 735 m (ring deformation), 613 s (M–O) and 512 m (M–N). ^{1}H NMR (DMSO-d_6, 300 MHz): δ = 3.36 (s, 1H, H-5), 4.74 (s, 2H, H_2O), 7.26 (s, 2H, NH_2), 7.28(d, 1H, *J* = 3.6 Hz, thienyl-C_3'H), 7.94 (dd, 1H, *J* = 3.5, thienyl-C_4'H), 8.11 (d, 1H, *J* = 5.2 Hz, thienyl-C_5'H), 10.85 (s, 1H, N–H coordinated) and 12.12 (3) (s, 1H, N–H free).

In vitro antimicrobial activities and minimum inhibition concentration (MIC)

The antimicrobial activities of the L_1, L_2 ligand and its complexes were evaluated using the agar well diffusion method [18–20] against different bacterial strains such as Gram-positive (*Staphylococcus aureus*), Gram-negative (*Escherichia coli*), furthermore versus various fungal species like *A. fumigatus* and *G. candidum*. Mueller–Hinton agar medium (20 mL) was poured into each Petri plate, and the agar plates were swabbed with 100 µL inocula of each test bacterium and fungus and kept for 15 min for adsorption. Using a sterile cork borer of 6 mm in diameter, the wells were bored into the seeded agar plates and these were loaded with a 100-µL volume with a concentration of 1.25, 2.50 and 5.00 mg mL^{-1} of each compound reconstituted in methanol. All the plates were incubated at 37 °C for 24 h. Antibacterial and antifungal activities, indicated by an inhibition zone surrounding the wells containing the compounds, were recorded if the zone of inhibition was greater than 6 mm. The experiments were performed in triplicate. DMSO was used as a negative control, whereas cephalexin (5 mg mL^{-1}) was used as a positive control. The microdilution broth susceptibility assay was used for the evaluation of the minimal inhibitory concentration (MIC). After incubation at 37 °C for 24 h, the first tube without turbidity was determined as the MIC [23].

Protease inhibitory assay

Stock solutions of each of the compounds (L_1, L_2 and its Mn(II) complexes) were prepared by dissolving in DMSO. Each compound was prepared at concentration (0.001 M). An appropriate control was prepared using DMSO and protease only, and the effect of DMSO on protease activity was taken into account. For the protease assay, compounds were

preincubated at 37 °C with the enzyme for 1 h before the addition of substrate. And the residual activity was measured. The protease activity of the synthesized compounds was monitored at 750 nm in a 20 D spectrophotometer. The activity of the enzyme in the absence of the tested compounds and inhibitors was taken as 100%. The protease strain was isolated and indentified using the Biolog Microlog™ 34.20 database software (Biolog, Hayward, CA) at the Unit of Microorganisms Identification and Biological Control of the Agriculture Research Centre [28–31].

Results and discussion

Chemistry of organic compounds

In this article, we want to illustrate the use of Mn_2O_3 as a nano- and green solid acid catalyst in the synthesis of 7-amino-4-oxo-5-(thiophen-2-yl)2*H*-pyrano[2,3-*d*] pyrimidine-6-carbonitrile derivatives **1-1a** by the Knoevenagel–Michael condensation reaction. The procedure composed of the mixture of malononitrile, thiophene-2-carbaldehyde and barbituric acid derivatives in ethanol. To optimization manner on Mn_2O_3 catalysis and pyrano-pyrimidine heterocyclic synthesis by the effect of catalyst amount of Mn_2O_3 nanocatalyst on the reaction yield found 1 mmol of Mn_2O_3 yielded around 80% in 30 min of pyrano-pyrimidine is the optimized to complete the reaction. Also, comparing the efficiency of ethanol, several solvents with different polarities were tested; it was found that ethanol is the effective solvent for this study. The reaction goes ahead in high yields in the presence of Mn_2O_3 as catalyst at room temperature to obtain our coveted products **1-1a** (Scheme 1).

The 7-amino-2,3,4,5-tetrahydro-4-oxo-5-(thiophen-2-yl)-2-thioxo-1H-pyrano[2,3-d]pyrimidine-6-carbonitrile **1a** was used as starting materials. It contains an amino and a cyano group in adjacent positions, which is required for the synthesis of the condensed systems including pyrimidine. It has been found that by the reaction of compound **1** with malononitrile in refluxing ethanolic sodium ethoxide solution we obtained [6-amino-4-oxo-2-sulfanylidene-5-(thiophen-2-yl)-1,3,4,5-tetrahydro-2*H*-pyrano[2,3-*d*:6,5-*d'*] dipyrimidin-8-yl]acetonitrile (2), respectively. The ^{1}H NMR spectrum of compound **2** revealed a methylene singlet at d 4.17 ppm besides other signals attributable to an aromatic compound and only one NH_2 group at 8.0 ppm as expected (cf. "Experimental"). Based on these data, it seemed that a $–CH_2CN$ side chain is present. Similar cyclizations with other nitriles have been reported [32].

The pyrano pyrimidinone derivative **3** was procreated by refluxing compound **1** in excess formic acid. The IR spectrum of compound **3** substantiated the absorption bands of pyrimidinone NH and C=O, respectively, at their prospective values. ^{1}H NMR and elemental analysis gave the confirmatory data for compound **3** (cf. Scheme 2 and "Experimental" section).

Treatment of compound **1** with cold concentrated sulfuric acid portionwise and sanitizing on an ice bath for about an hour given the pyrano carboxamide derivative **4**. IR spectrum of compound **4** substantiated absorption bands at 3431 for pyrano NH_2, 3162 for amide NH_2, 3114 for pyrimidine NH and 1671,1645 for (2C=O); its ^{1}H NMR displayed three singlets at δ 8.48, 9.14 and 12.37 ppm for (D_2O exchangeable) pyrano NH_2, amide NH_2 and pyrimidine NH, respectively.

The 5-amino pyrano[2,3-*d*]pyrimidine 4-carbonitrile derivative **1** was found to be an sufficient, key starting for the synthesis of some other new heterocyclic compounds, where it was heated in formamide for 3 h, to produce compound **5**. The structure of compound **5** was confirmed by its spectral and analytical data.

Continuing a series of synthesis the pyrano carboxamide derivative **4** was transformed into the pyrano triazinone **7** by the addition of sodium nitrite solution to a suspended solution of **4** in concentrated hydrochloric acid at 0–5 °C with stirring at room temperature. Structure of compound **7** was approved by IR, ^{1}H NMR elemental analysis (cf. Scheme 3 and "Experimental" section).

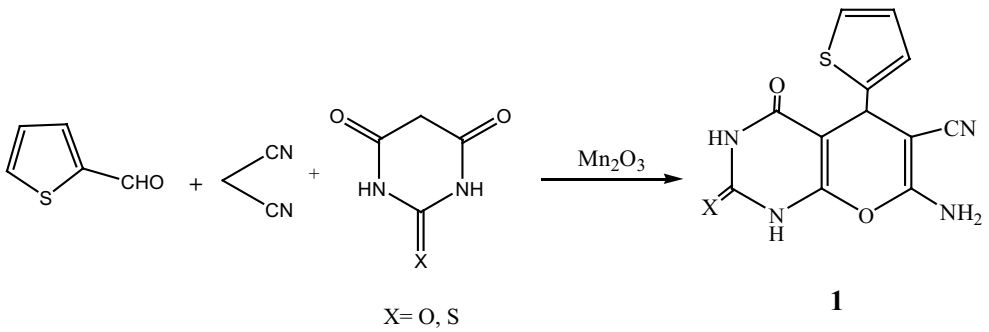

Scheme 1 Synthesis of pyrano[2, 3-*d*]pyrimidine derivatives

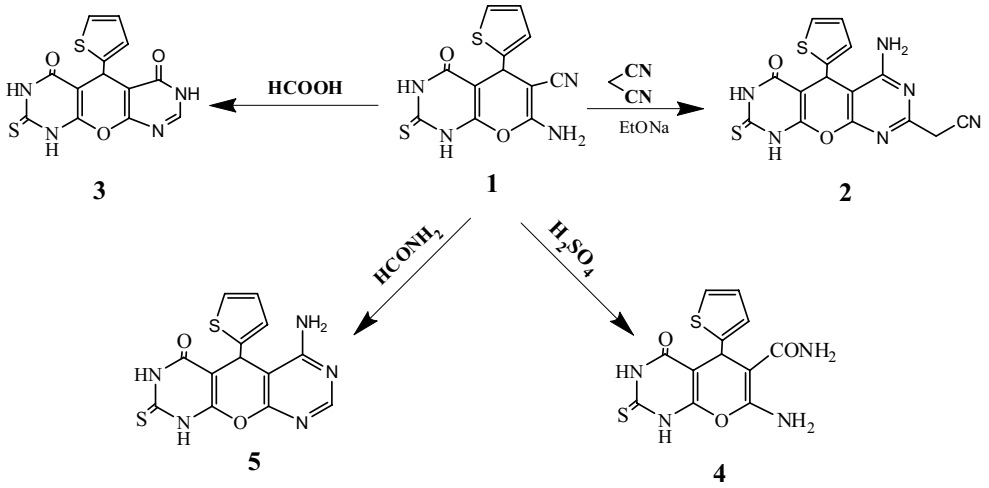

Scheme 2 Heterocyclization reactions

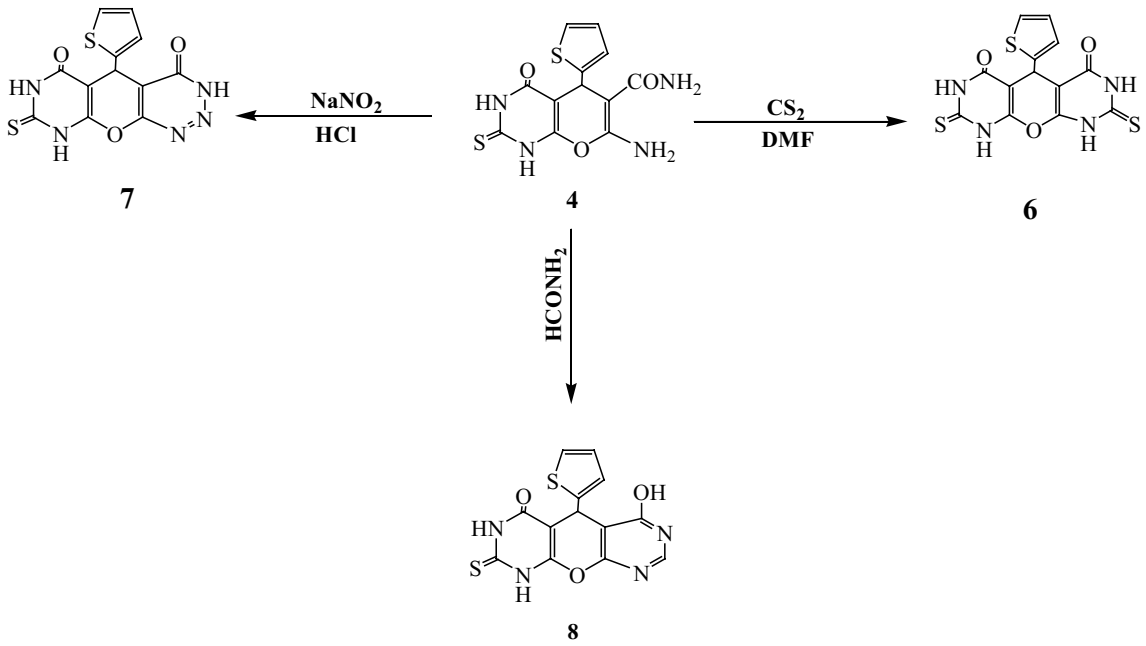

Scheme 3 Synthesis of fused pyrimidine derivatives

Refluxing a solution of compound **4** in dimethylformamide with 20% potassium hydroxide solution and carbon disulfide (5 mL) afforded the thioxopyrano pyrimidinone derivative **6**, which structure was deduced from its analytical and spectral data; boiling compound **4** in formamide afforded the 4-hydroxypyrano[3,4- *d*]pyrimidine **8** (cf. "Experimental" section) (Scheme 3).

Physical measurements data

Mn(II) L_1 and L_2 complexes were synthesized as solids of a color characteristics of the metal ion. The results obtained indicate that all of the isolated complexes are formed from the reaction of the metal salt with free ligands in 1:1 molar ratio for all the elements. All of the complexes reported here

are air stable solids at room temperature. The structures of the complexes suggested from the elemental analysis agree quite well with their proposed formulas. The found values of elemental analysis agree quite well with the calculate percentage of C, H, N, Cl and sulfur. The metal content is a well agreement with the molecular formulas of the prepared complexes. The biological activity of ligands and its metal chelates are studied against some selected Gram-positive, Gram-negative bacteria, two species of fungi and protease inhibitory activity.

Molar conductance measurements

Conductivity measurements have frequently been used to predict the structure of metal chelates within the limits of their solubility. They provide a method of testing the degree of ionization of the complexes, the molecular ions that a complex liberates in solution (in case of presence of anions outside the coordination sphere); the higher will be its molar conductivity and vice versa [33, 34]. The molar conductance values for the L_1, L_2 and its complexes in DMSO solvent at $1.0 \times 10P^{-3}$ M are consistent with the nonelectrolyte nature (5.97, 5.99, 6.00, 6.66 μS cm^{-1}) of the compounds at room temperature [33, 34]. The obtained results were strongly matched with the elemental analysis and experimental data.

Infrared spectral data

The ultimate substantial infrared bands for the L_1, L_2 ligands and its complexes together with their assignments are shown in Fig. 1, and the assignments are given in Table 1. The infrared spectra of the two complexes are compared with those of the free ligands in order to determine the site of coordination that may be involved in chelation. There are some guide peaks in the spectrum of the ligand which are of good help for achieving this goal. These peaks are expected to be involved in chelation. The position or the intensities of these peaks are expected to be changed upon complexation. A comparison of the IR spectra of the ligands with those of the metal complexes showed that the spectra of the complexes exhibited broad bands in the range of 3545–3341 cm^{-1} which may be attributed to the ν(O–H) vibration of the water molecules. While the band observed at 889, 839 cm^{-1} can be assigned to coordinated water molecules (Scheme 4), this was confirmed by the results of thermal analysis [35, 36].

In the spectrum of free L_1 ligand, the bands observed at 3146, 3049 and 1677 cm^{-1} have been assigned to the stretching vibration of the two ν(–N–H) and two carbonyl groups ν(C=O) [37–39]. The shift of the characteristic bands of one (–N–H) and two carbonyl groups to a lower values at 3100 and 1654 cm^{-1} indicates the involvement of two carbonyl group and one nitrogen of the N–H group in the

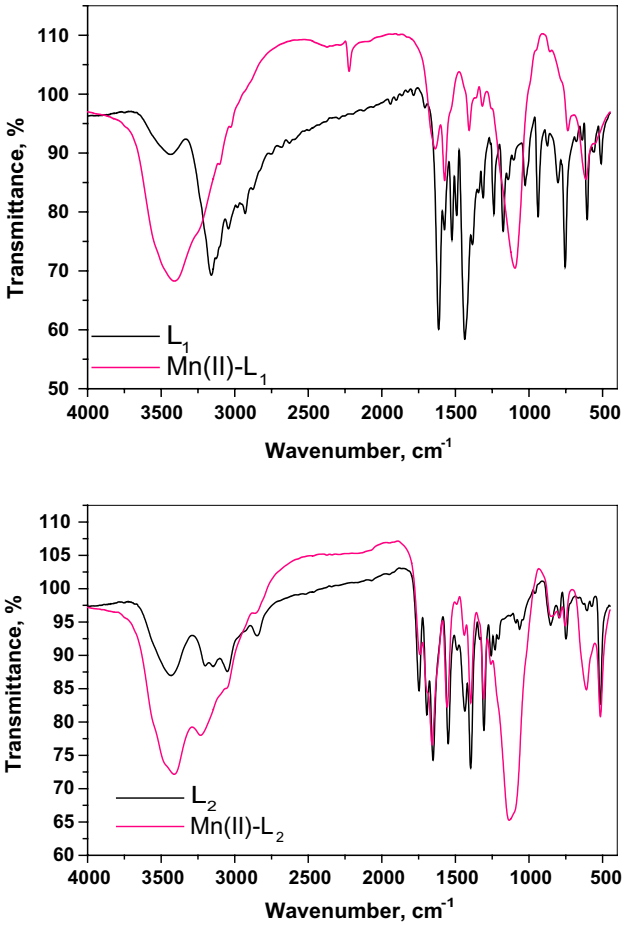

Fig. 1 Infrared spectra of L_1, L_2 ligands and its Mn(II) complexes

Table 1 IR frequencies (cm^{-1}) of L_1, L_2 and its complexes

Assignments	Compounds			
	L_1	[Mn(L_1) $Cl_2(H_2O)$]	L_2	[Mn(L_2) $Cl_2(H_2O)$]
ν(NH_2)	3431	3431	3490	3490
	3200	3200	3385	3385
ν(N–H)				
Coordinated	3146	3100	3174	3150
Free	3049	3049	3174	3174
ν(–CN)	2228	2228	2222	2222
ν(C = O	1677	1654	1694	1664
ν(C = S)	–	–	1256	1230
H_2O stretch of coordinated water	–	889	–	839
ν(M–O)	–	609	–	613
ν(M–O) stretch of coordinated water	–	589	–	578
ν(M–N)	–	515	–	512

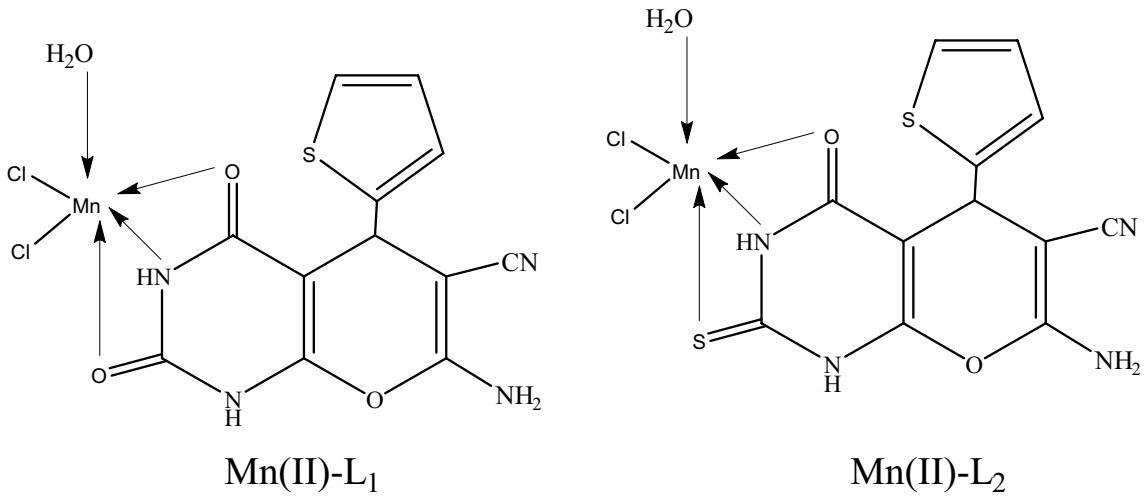

Scheme 4 The proposed coordination mode of Mn(II) with L_1 and L_2

interaction with metal ion, i.e., L_1 acts as tridentate ligand through (ONO) [40].

In the spectrum of free L_2 ligand, the bands observed at 3174, 1694 and 1256 cm^{-1} have been assigned to the stretching vibration of the two ν(–N–H), carbonyl ν(C=O) and ν(C=S), respectively [41]. The shift of the characteristic bands of one N–H, C=O and C=S to a lower values at 3150, 1664 and 1230 cm^{-1} indicates the involvement of these three groups in chelation with Mn(II), i.e., L_2 reacts as tridentate ligand through (ONS) [40].

The spectra of the isolated solid complexes show two of bands with different intensities which characteristics for (M–N) and (M–O). The ν(M–N) and ν(M–O) bands observed at 609, 515 cm^{-1} for Mn(II)–L_1 and 613, 512 cm^{-1} for Mn(II)–L_2 (Table 1) are absent in the spectrum of free ligands. The proposed structure formulae on the basis of the IR results are presented in Scheme 4.

Electronic spectra

The electronic absorption spectra of L_1, L_2 ligands and its Mn(II) complexes from 200 to 800 nm are shown in Fig. 2 and Table 2. Free ligands show two essential absorption bands at 330 and 412 nm, which may be assigned to π–π* and n–π* transitions, respectively [42]. These transitions were existed also in the spectra of the complexes, but they shifted to higher values, confirming the coordination of the ligand to the metal ions. In UV–Vis spectra, the weak band should be at 492 nm due to ligand–Mn(II) charge transfer (CT) band in the complexes, which is absent in the free ligands. However, the weak broad band at 578 nm is due to different *d*–*d* transitions of the metal ions as mentioned [43]. Information concerning the geometry of these compounds was obtained from the electronic spectra and from magnetic

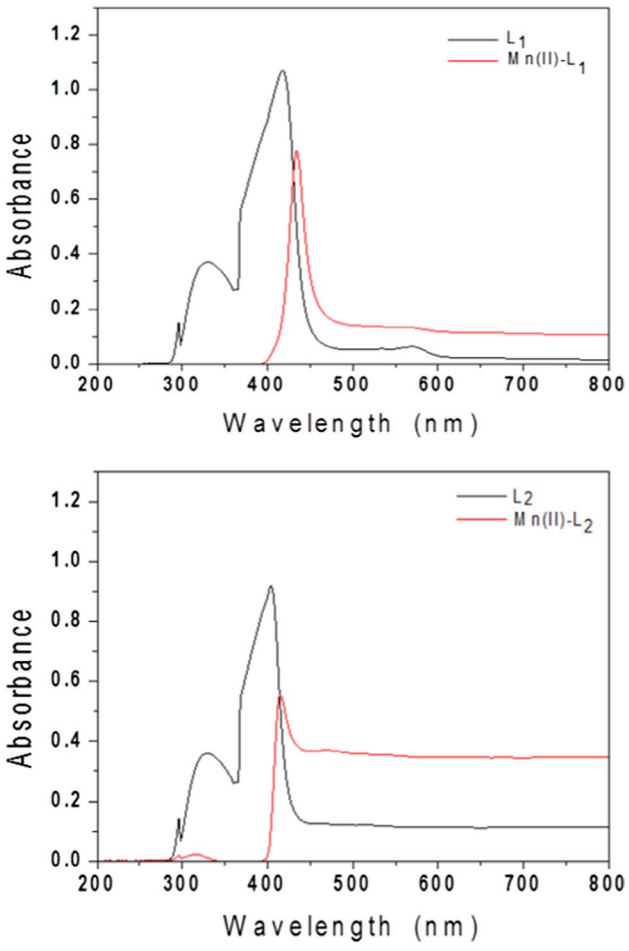

Fig. 2 Electronic absorption spectral data of L_1, L_2 ligands and its Mn(II) complexes

Table 2 Spectrophotometric determination of L_1, L_2 ligands and its Mn(II) complexes

Compounds	λ_{max} (nm)	Molar absorptivity (ε_{max}) $L{\cdot}mol^{-1}{\cdot}cm^{-1}$	Assignments
L_1	330	360	π–π^* transitions
	412	919	n–π^* transitions
Mn(II)–L_1	420	503	π–π^* transitions
	432	394	n–π^* transitions
	492	363	L Mn(II) CT
	578	348	*d*–*d* transitions
L_2	330	370	π–π^* transitions
	412	1072	n–π^* transitions
Mn(II)–L_2	428	563	π–π^* transitions
	434	780	n–π^* transitions
	492	146	L Mn(II) CT
	578	131	*d*–*d* transitions

moment values. The electronic spectrum of the Mn(II) complexes shows four medium intensity bands assigned to $6A_{1g} \rightarrow 4T_{1g}(G)$, $6A_{1g} \rightarrow 4T_{2g}(G)$ and $6A_{1g} \rightarrow 4E_g(G)$, $4A_{1g}(G)$, respectively, for a Mn(II) ion in an distorted octahedral field [44].

Magnetic measurements

The magnetic susceptibility measurements thus help to predict the possible geometry of the metal complexes. In paramagnetic Mn(II) complexes, often the magnetic moment (μ_{eff}) gives the spin-only value ($\mu_{s.o.} = (n(n+2))^{1/2}$ B.M.) corresponding to the number of unpaired electron. The variation from the spin-only value is attributed to the orbital contribution, and it varies with the nature of coordination and consequent delocalization. The magnetic moment, configurations, stereochemistry, hybrid orbitals, number of unpaired electrons and expected magnetic values of Mn(II) complexes are (5.97 B.M., d^5, octahedral, sp^3d^2, 5, 6.00 B.M.), respectively. Thus, the value of magnetic moment of a complex would give valuable insights into its constitution and structure. The magnetic moment lies within the region expected for octahedral complexes [44].

Thermal studies

Confirming the proposed structures of the complexes $[Mn(L_1)(H_2O)Cl_2]$ and $[Mn(L_2)(H_2O)Cl_2]$ thermogravimetric (TG) and differential thermogravimetric (DTG) analyses were studied (Table 3 and Fig. 3). The proposed mechanisms for the thermal decomposition of L_1, L_2 and its complexes were only based on speculation.

Thermal results reveal that the decomposition of L_1 occurs in one degradation stage. In addition, deep investigation of the ligand decomposition reveals that this decomposition occurs at three maxima: 315, 374 and 756 °C, with total weight loss of 82.89% corresponding to the loss of $4C_2H_2 + 2N_2O + S_2O$, leaving 4C as a residual product with a percentage of 17.11%. The decomposition for the $[Mn(L_1)(H_2O)Cl_2]$ complex exhibits one main degradation steps at 174, 270, 408 and 509 °C with a weight loss of 81.92%, in good agreement with the calculated value 81.73%, corresponding to the loss of $5C_2H_2 + 2N_2O + S_2O + Cl_2$ giving the decomposition product MnO(NPS) + 2C.

L_2 exhibits approximately one step at 300, 491 and 745 °C which is accompanied by a mass loss of 88.30% corresponding to the loss of $4C_2H_2 + 2N_2 + S_2O + CO$, leaving 3C as a residual product with a percentage of 11.70% (Calc. 11.82%). $[Mn(L_2)(H_2O)Cl_2]$ complex decomposed in one stage at 287, 539 and 718 °C which are accompanied by a weight loss of 81.08%; these are attributed to the loss of $5C_2H_2 + 2N_2 + S_2O + Cl_2 + CO$ giving MnO(NPS) + C as a final product.

The MnO (NPS) properties were studied with the help of a scanning electron microscope (SEM). Figure 4 shows the SEM image of the synthesized MnO (NPS), with an image magnification. The assembly was attached to a computer running a program to analyze the mean size of the particles in the samples. It should be noted that the

Table 3 Maximum temperature T_{max} (°C) and weight loss values of the decomposition stages for L_1, L_2 ligands and its Mn(II) complexes

Compounds	Decomposition	T_{max} (°C)	Weight loss (%)		Assignment
			Calc.	Found	Lost species
L_1	First step	315, 374, 756	83.35	82.89	$4C_2H_2 + 2N_2O + S_2O$
$C_{12}H_8N_4O_3S$	Residue		16.65	17.11	4C
$[Mn(L_1)(H_2O)Cl_2]$	First step	174, 270, 408, 509	81.73	81.92	$5C_2H_2 + 2N_2O + S_2O + Cl_2$
$MnC_{12}H_{10}N_4O_4SCl_2$	Residue		18.26	18.08	MnO + 2C
L_2	First step	300, 491, 745	88.17	88.30	$4C_2H_2 + 2N_2 + S_2O + CO$
$C_{12}H_8N_4O_2S_2$	Residue		11.82	11.70	3C
$[Mn(L_2)(H_2O)Cl_2]$	First step	287,539,718	81.49	81.08	$5C_2H_2 + 2N_2 + S_2O + Cl_2 + CO$
$MnC_{12}H_{10}N_4O_3S_2Cl_2$	Residue		18.50	18.92	MnO + C

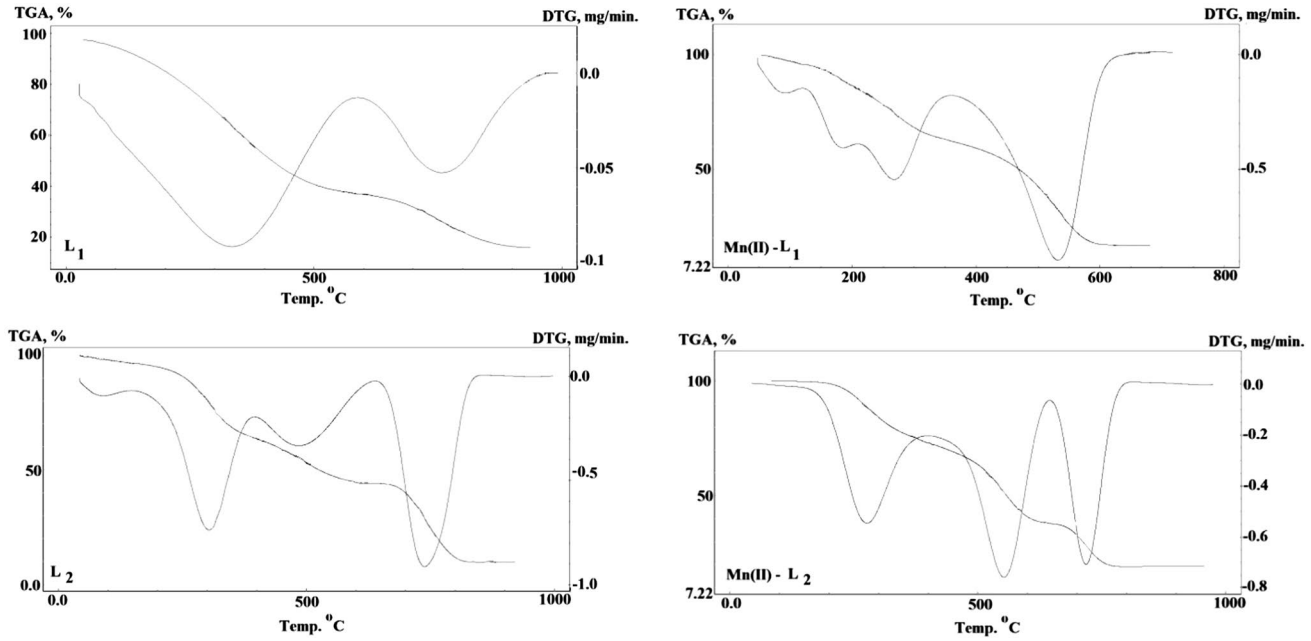

Fig. 3 TGA and DTG diagrams for L_1, L_2 and its complexes

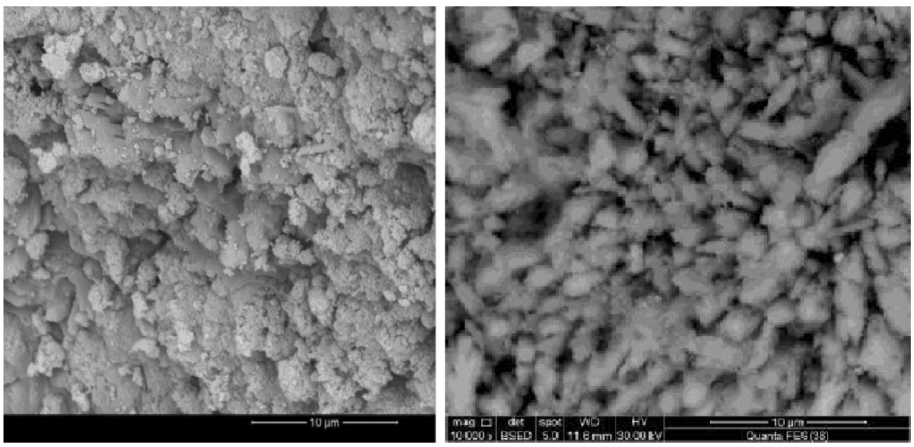

Fig. 4 SEM images of synthesized MnO nanoparticles using $[Mn(L_1)(H_2O)Cl_2]$ and $[Mn(L_2)(H_2O)Cl_2]$ complex precursors at 600 °C

particle diameter is always overestimated due to the distortion of SEM images [45]. The results of nanoparticle size measurement of samples (the morphology) by XRD, SEM (SEM studies showed that the particle size ranged from 100 to 540 nm) and TEM (Fig S1, TEM studies showed that the particle size ranged from 90 to 250 nm) indicate that the size of the MnO nanoparticles was 100 and 250 nm which is larger than the nanoparticle size. It is noteworthy that based on the thermal analysis data, the proposed formulae of the complexes under investigation could be confirmed.

Antimicrobial activities and minimum inhibitory concentration (MIC)

The susceptibility of certain strains of bacterium, such as *Staphylococcus aureus* (*S. aureus*), *Escherichia coli* (*E. coli*) and antifungal screening, was studied against two species *G. candidum* and *A. Fumigates* toward the free ligands and its complexes were judged by measuring size of the zone of growth inhibition and minimal inhibitory concentrations. As assessed by color, the complexes remain intact during biological testing (Table 4). A comparative

Table 4 Averages of inhibition growth diameter (mm) of the ligands, complexes and standards, obtained via a disk diffusion method in three concentrations (1.25, 2.5 and 5 mg mL^{-1}) against selected Gram-positive, negative bacteria and two fungi strains

Compounds	Microorganisms											
	Fungi						Gram-positive bacteria			Gram-negative bacteria		
	A. fumigatus			*G. candidum*			*S. aureus*			*E. coli*		
	1.25	2.5	5	1.25	2.5	5	1.25	2.5	5	1.25	2.5	5
L_1	5 ± 0.1	7.5 ± 0.1	10 ± 0.1	10 ± 0.05	12.5 ± 0.05	15 ± 0.05	21 ± 0.08	23 ± 0.08	25 ± 0.08	7 ± 0.45	9 ± 0.45	11 ± 0.45
Mn(II)–L_1	$13^{+2} \pm 0.84$	$19^{+3} \pm 0.84$	$25^{+3} \pm 0.84$	$19^{+1} \pm 0.35$	$25^{+2} \pm 0.35$	$28.5^{+3} \pm 0.35$	$25^{+1} \pm 0.58$	$27.5^{+1} \pm 0.58$	$30.5^{+1} \pm 0.58$	$18^{+2} \pm 0.57$	$25.6^{+3} \pm 0.57$	$29^{+3} \pm 0.57$
L_2	3 ± 0.68	6 ± 0.68	9.67 ± 0.68	4.5 ± 0.54	7 ± 0.54	9 ± 0.54	15 ± 0.36	20.66 ± 0.36	24.45 ± 0.36	6.6 ± 0.04	9 ± 0.04	14.5 ± 0.04
Mn(II)–L_2	$11.1^{+1} \pm 0.2$	$15.61^{+2} \pm 0.2$	$21^{+3} \pm 0.2$	$16.3^{+3} \pm 0.05$	$19.5^{+3} \pm 0.05$	$26.2^{+3} \pm 0.05$	$21.4^{+1} \pm 0.03$	$28.5^{+1} \pm 0.03$	$36^{+2} \pm 0.03$	$17.2^{+2} \pm 0.2$	$24.4^{+3} \pm 0.2$	$28.5^{+3} \pm 0.2$
Mn(II)	NA	NA	NA	NA	NA	NA	13 ± 0.04	15 ± 0.04	16.5 ± 0.04	5 ± 0.15	7 ± 0.15	8.88 ± 0.15
Cephalexin	NA	NA	NA	NA	NA	NA	NA	NA	25.81	NA	NA	28.5

Data are expressed in the form of mean ± standard deviation (SD)

NA no activity

Statistical significance P^{NS} *P* not significant, $P < 0.05$; P^{+1} *P* significant, $P > 0.05$; P^{+2} *P* highly significant, $P > 0.01$; P^{+3} *P* very highly significant, $P > 0.001$; Student's *t* test (paired)

Table 5 Minimum inhibitory concentration [MIC, (μg mL^{-1})] against selected Gram-positive, negative bacteria and fungi species

Compounds (mg mL^{-1})	Microorganisms			
	Fungi		Gram-positive bacteria	Gram-negative bacteria
	A. fumigatus	*G. candidum*	*S. aureus*	*E. coli*
L_1	7.5	5	5	5
Mn(II)–L_1	2.5	1.25	1.25	2.5
L_2	10	5	10	5
Mn(II)–L_2	5	2.5	1.25	2.5

study of ligand and their metal complexes showed that the metal complexes exhibit higher antibacterial and antifungal activities. The highly effect of complexes can be elucidated on the principle of cell permeability; the lipid membrane around the cell supports the permeation of lipid-soluble substances; liposolubility is remarkable factor that controls the antimicrobial activity. On complexation the polarity of the metal ion will be reduced due to overlap of ligand orbital and partial sharing of the positive charge of the metal ion with donor groups [23, 41]. It is likely that the increased liposolubility of the ligand upon metal chelation may participate to its easy transport into the bacterial cell which blocks the metal-binding sites in enzymes of microorganisms [23]. The order of drug potencies decreases in: Mn(II)–L_1 > Mn(II)–L_2 > L_1 > L_2 > L_1 > Mn(II), Mn(II)–L_1 > Mn(II)–L_2 > L_1 > L_2 in case of bacterial and fungi species, respectively. Such an increased activity of metal chelate can be explained on the basis of the oxidation state of the metal ion, overtone concept and chelation theory [41–48]. The quantitative assays gave MIC values in the region 1.25–10 μg mL^{-1} (Table 5), in agreement with the above-obtained results.

Novel protease inhibitors

Protease is a retroviral aspartyl protease that is essential for the life cycle of HIV, the retrovirus that causes AIDS [49, 50]. There has been a considerable interest for development of synthetic inhibitors for this enzyme, with low molecular weights and minimal peptide characters. For this we have been developed a novel compound with aim to be new protease inhibitors. L_1, L_2 and its Mn(II) complexes (PIS) can be used as antiviral drugs to treat HIV/AIDS and hepatitis caused by hepatitis C virus. Thus, mutation of protease's active site or inhibition of its activity disrupts its ability to replicate and infect additional cells, making inhibition the subject of considerable pharmaceutical research. The effects of L_1, L_2 and its Mn(II) complexes on the enzyme activity are summarized in Table 6 and Fig. 5. Maximum enzyme inhibition was achieved

Table 6 The effects of protease inhibitors (L_1, L_2 and its Mn(II) complexes) on the enzyme activity

Inhibitor	Volumes[a] (1 = 50 µL) (PIS:P)	Relative activity (%)
None	0:01	100.0 ± 2.5
L_1	1:01	76.0 ± 1.9
	2:01	64.0 ± 1.6
	10:01	0.0
Mn(II)–L_1	1:01	60.0 ± 1.5
	2:01	56.0 ± 1.4
	10:01	0.0
L_2	1:01	88.0 ± 2.2
	2:01	80.0 ± 2.0
	10:01	0.0
Mn(II)–L_2	1:01	68.0 ± 1.7
	2:01	64.0 ± 1.6
	10:01	0.0

PIS:P protease inhibitors: protease enzyme

[a]Concentration of PIS (1.0 mM)

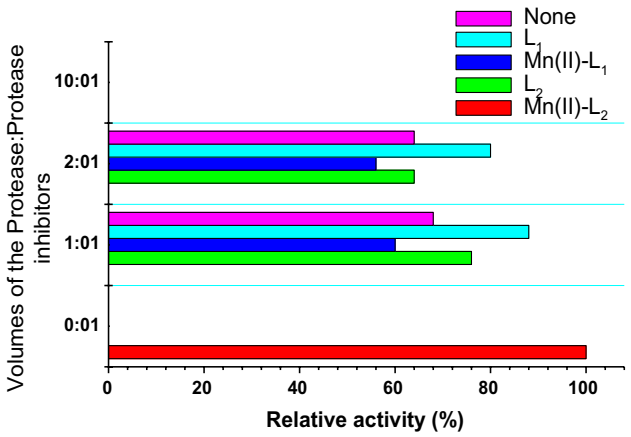

Fig. 5 Statistical representation for protease inhibitors

with Mn(II)–L_2 complex. L_1, L_2 compounds exhibited a significant effect on the activity. However, the Mn(II)–L_1 highly repressed the enzymatic activity. The enzyme activity was almost completely lost by all compounds in case of using the ratio of one protease enzyme to ten PIS compounds during incubation period. The order of protease inhibitors decreases in: Mn(II)–L_1 > Mn(II)–L_2 > L_1 > L_2 > L_1.

Conclusion

In the present work, new pyrano[2,3-*d*] pyrimidine derivatives as ligands and its Mn(II) complexes with the general formula [Mn(L_n)(H_2O)Cl_2] (n = 1 or 2) were synthesized. The obtained evidence of UV–Vis and magnetometry can support the octahedral geometries for the complexes. The results of the elemental analysis, thermal analysis, spectroscopic studies, molar conductivity and magnetic moment deduced the formation of 1:1 metal/ligand complexes in all cases. In addition, the investigation of the biological activity of the ligands and their manganese complexes shows the acceptable prevention of these compounds against some selected strains of bacteria and fungi as well as its protease inhibition. Finally, the Mn(II) complexes are air stable and soluble in polar solvents.

Acknowledgements The authors gratefully acknowledge the Central Laboratory of Medicine Ministry for performing the antimicrobial measurements and Institute of Science and Nanotechnology in Kafr El Sheikh for synthesis the Mn_2O_3 nanoparticles.

References

1. L. Weber, Curr. Med. Chem. **9**, 2085 (2002)
2. A. Mobinkhaledi, M.A. Bodaghi Fard, Acta Chim. Slov. **57**, 931 (2010)
3. G.L. Anderson, J.L. Shim, A.D. Broom, J. Org. Chem. **41**, 1095 (1976)
4. E.M. Grivsky, S. Lee, C.W. Sigel, D.S. Duch, C.A. Nichol, J. Med. Chem. **23**, 327 (1980)
5. D. Heber, C. Heers, U. Ravens, Die Pharm. **48**, 537 (1993)
6. Y. Sakuma, M. Hasegawa, K. Kataoka, K. Hoshina, N. Kadota, Chem. Abstr. **115**, 71646 (1991)
7. C. Musstazza, M.R.D. Guidice, A. Borioni, F. Gatta, J. Heterocycl. Chem. **38**, 1119 (2001)
8. I. Devi, P.J.Bhuyan Kumar, Tetrahedron Lett. **44**, 8307 (2003)
9. Y. Gao, S. Tu, T. Li, X. Zhang, S. Zhu, F. Fang, D. Shi, Synth. Commun. **34**, 1295 (2004)
10. T.S. Jin, L.B. Liu, S.J. Tu, Y. Zhao, T.S. Li, J. Chem. Res. **3**, 162 (2005)
11. R.S. Hamid, S. Mohsen, R. Sudabeh, S. Athar, Green Chem. **14**, 1696 (2012)
12. A. Maleki, M. Kamalzare, Catal. Commun. **53**, 67 (2014)
13. A.R. Bahat, A.H. Shalla, R.S. Dongre, J. Saud. Chem. Soc. **2014**, 4 (2014)
14. A. Shaabani, M. Seyyedhamzeh, A. Maleki, F. Rezazadeh, M. Behnam, J. Comb. Chem. **11**, 375 (2009)
15. A. Maleki, A. AliJafari, S. Yousefia, Carbohydr. Polym. **175**, 409 (2017)
16. A. Maleki, R. Paydar, RSC Adv. **5**, 33177 (2015)
17. A. Maleki, P. Ravaghi, M. Aghaei, H. Movahed, Res. Chem. Intermed. **43**, 5485 (2017)
18. A. Maleki, S. Azadegan, Inorg. Nano Metal Chem. **47**, 917 (2017)
19. A. Maleki, S. Azadegan, J. Inorg. Organomet. Polym. **27**, 714 (2017)
20. A. Maleki, R. Rahimi, S. Maleki, J. Iran. Chem. Soc. **2**, 191 (2015)
21. A. Maleki, M. Aghaei, R. Paydar, J. Iran. Chem. Soc. **14**, 485 (2017)
22. A. Maleki, A.A. Jafari, S. Yousefi, J. Iran. Chem. Soc. **14**, 1801 (2017)
23. S.A. Sadeek, W.H. El-Shwiniy, J. Iran. Chem. Soc. **14**, 1711 (2017)
24. A.H. Moustafa, H.A. Saad, W.S. Shehab, M.M. El-Mobayed, Phosphorus Sulfur Silicon Relat. Elem. **183**, 115 (2007)
25. W.S. Shehab, Curr. Org. Chem. **13**, 14 (2009)

26. E.K. Mohamed, W.S. Shehab, J. Korean Chem. Soc. **55**, 988 (2011)
27. W.S. Shehab, E.K. Mohamed, Eur. J. Chem. **3**, 241 (2012)
28. H.L. Singh, J.B. Singh, K.P. Sharma, Res. Chem. Intermed. **38**, 53 (2012)
29. I. Ahmad, A.J. Beg, J. Ethnopharmacol. **74**, 113 (2001)
30. J.M. Andrews, J. Antimicrob. Chemother. **48**, 5 (2001)
31. E. Kotb, M.I. Abouel-Hawa, E.Y. Tohamy, K. El-Msalamy, Biologia **68**, 797 (2013)
32. N.R. Smyrl, R.W. Smithwick, J. Heterocycl. Chem. **19**, 493 (1982)
33. W.J. Geary, Coord. Chem. Rev. **7**, 81 (1971)
34. J. Devi, N. Batra, Asian J. Res. Chem. **6**, 960 (2013)
35. S.L. Stefan, B.A. El-Shetary, W.G. Hanna, S.B. El-Maraphy, Microchem. J. **35**, 51 (1987)
36. K. Nakamato, P.J. Mc Carthy, *Spectroscopy and Structure of Metal Chelate Compounds* (Wiley, New York, 1968), p. 268
37. H. Almodfa, A.A. Said, E.M. Nour, Bull. Soc. Chem. Fr. **128**, 137 (1991)
38. S.A. Sadeek, S.M. Teleb, M.S. Refat, M.A.F. Elmosallamy, J. Coord. Chem. **58**, 1077 (2005)
39. R.M. Silverstein, G.C. Bassler, T.C. Morril, *Spectroscopic Identification of Organic Compounds*, 5th edn. (Wiley, New York, 1991)
40. M.S. Refat, S.A. El-Korashy, A.S. Ahmed, Spectrochim. Acta Part A **71**, 1084 (2008)
41. F.D. Rochon, R. Melanson, J.P. Macouet, F. Belanger-Gariepy, A.L. Beauchamp, Inorg. Chim. Acta **108**, 17 (1985)
42. S.A. Sadeek, S.M. Abd El-Hamid, W.H. El-Shwiniy, Res. Chem. Intermed. **42**, 3183 (2016)
43. A.B.P. Lever, Coord. Chem. Rev. **3**, 119 (1968)
44. D.D. Bui, J. Hu, P. Stroeven, Cem. Concr. Compos. **27**, 357 (2005)
45. E. Mendez, M.F. Cerda, J.S. Gancheff, J. Torres, C. Kremer, J. Castiglioni, M. Kieninger, O.N. Ventura, J. Phys. Chem. **C111**, 3369 (2007)
46. M.S. Refat, S.A. El-Korashy, A.S. Ahmed, Spectrochim. Acta Part A **71**, 1084 (2008)
47. N.M. El-Metwaly, Trans. Metal Chem. **32**, 88 (2007)
48. D.R. Davies, Annu. Rev. Biophys. Biophys. Chem. **19**, 189 (1990)
49. A. Brik, C.H. Wong, Org. Biomol. Chem. **1**, 5 (2003)
50. X. Huang, M.D. Britto, J.L. Kear-Scott, C.D. Boone, J.R. Rocca, C. Simmerling, R. Mckenna, M. Bieri, P.R. Gooley, B.M. Dunn, G.E. Fanucci, J. Biol. Chem. **289**, 17203 (2014)